Variation of nuclear magnetic shielding with intermolecular interactions and rovibrational motion. VIII. ^{19}F in CF_3X

Cynthia J. Jameson
Department of Chemistry, University of Illinois at Chicago, Chicago, Illinois 60680

A. Keith Jameson
Department of Chemistry, Loyola University, Chicago, Illinois 60626

(Received 22 February 1984; accepted 4 April 1984)

We have determined the effects of intermolecular interactions on the ^{19}F nuclear shielding for the series of fluorinated methanes CF_3X, X = H, F, Cl, Br, I, and the pseudohalide CN. The second virial coefficient of nuclear shielding, obtained from measurements of the ^{19}F nuclear resonance frequency in low density gas samples, corrected for bulk susceptibility effects, are: $(\sigma_1 - \sigma_{1b}) = -6.76, -8.65, -15.70, -17.19, -21.11$, and -30.1 ppb/amagat at 300 K varying systematically in the sequence X = H, F, Cl, CN, Br, and I. On the other hand, the temperature dependence of the ^{19}F shielding in the zero-pressure limit shows that at 300 K, $d\sigma_0/dt = -5.60, -5.01, -6.78, -7.45, -7.75$, *and* -9.25, for X = H, F, Cl, CN, Br, and I, respectively.

INTRODUCTION

Significant progress has been made in characterizing the ^{19}F nuclear magnetic shielding in the series of trifluoromethyl halides CF_3X, X = F, Cl, Br, and I, to which one may also add for comparison, X = H and the pseudohalide CN. The full ^{19}F shielding tensors have been measured.[1-3] *Ab initio* quantum-mechanical calculations of the ^{19}F shielding for X = H, F, Cl, and CN have been reported. These calculations with 6-311G basis sets using Ditchfield's GIAO method[4] give isotropic absolute shielding values of 302.6, 264.2, 265.3, and 274.8 ppm respectively,[5] whereas our absolute shielding scale studies give 274.1, 259.0, 224.4, and 252.1 ppm, respectively.[6,7] The calculations reproduce neither the order of chemical shifts nor the absolute shielding values. This series of molecules is well suited for a comparative study since differences between the ^{19}F shielding in these molecules should depend entirely on the changes produced by the substituent X. There is good evidence that the geometry of the CF_3 group in the molecules CF_4, CF_3H, CF_3Cl, CF_3Br, CF_3I, and CF_3CN is the same. Microwave spectroscopy[8,9] and electron diffraction data[10] agree with those from analysis of ^{19}F NMR rigid lattice line shapes.[1] In each molecule the C–F bond distance is 1.33 ± 0.01 Å and the FCF angle differs from tetrahedral by no more than 1°.

The nearly identical equilibrium geometry of the CF_3 group in these molecules makes a comparative study of the rovibrational averaging of the ^{19}F nuclear shielding meaningful. We have previously reported the temperature dependence of an "isolated" CF_3X molecule, for X = H, F, Cl, and Br.[11,12] The temperature dependence due to rovibrational averaging of the ^{19}F shielding in these molecules can be interpreted in terms of an electronic factor which is a measure of the change in nuclear shielding with C–F bond extension, and a dynamic factor which is a measure of the average C–F bond extension with increasing temperature. By making a comparative study of the members of the series, including CF_3I and CF_3CN, we hope to have a better understanding of the electronic factor. *Ab initio* calculations cannot give us theoretical values for these quantities just yet, since there are still difficulties in reproducing the average shielding at the equilibrium configuration. However, the success of some recent efforts in calculations of σ for ^1H and ^{13}C in molecules as large as benzene[13] and adamatane[14] indicate that ^{19}F shielding tensors may be calculated theoretically to the same accuracy in the near future.

The other aspect of our interest in this series of molecules is in the intermolecular effects. The different polarizabilities of the X atom in these molecules should lead to a systematic change in the effects of intermolecular interactions on ^{19}F shielding. In addition, the systematic change in mass in going from H to I may likewise lead to differences in intermolecular effects on shielding with respect to collisions

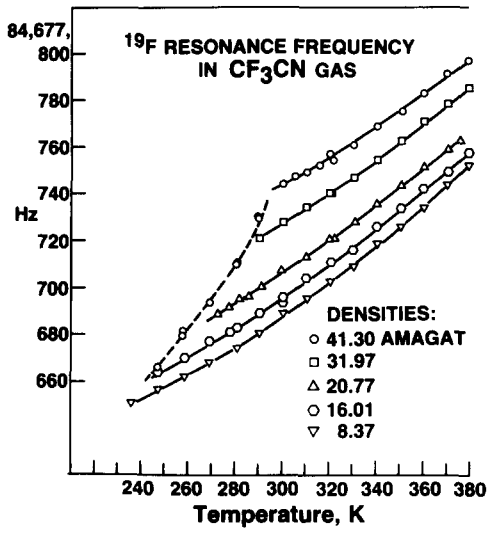

FIG. 1. Typical raw data obtained in temperature-dependent measurements of ^{19}F nuclear resonance frequencies in gas samples of various densities. The all-gas curves are not exactly parallel indicating a sizeable temperature dependence in σ_1. For temperatures below the condensation temperatures of various samples, the resonance frequency in the vapor is the same for all samples at the same temperature. The sharp drop in resonance frequency with decreasing temperature in the vapor phase is expected from the decrease of vapor pressure with decreasing temperature.

 0021-9606/84/151198-05$02.10

TABLE I. The observed second virial coefficient of ^{19}F nuclear shielding in various CF_3X gases $\sigma_1(T)$ and $(\sigma_1 - \sigma_{1b})$ for interaction between like pairs of CF_3X molecules in ppb/amagat.

Molecule	T(K)	$\sigma_1(T)$	χ, 10^{-6} cm^3 mol^{-1}	σ_{1b}	$(\sigma_1 - \sigma_{1b})$ at 300 K
CF_3H	240–380	$-(9.40 \pm 0.67) + 4.00\times10^{-2}(T-300) + 2.67\times10^{-4}(T-300)^{2}$[a]	-28.3[c]	-2.64	-6.76
CF_4	270–410	$-(11.55 \pm 0.31)$[b]	-31.0[d]	-2.90	-8.65
CF_3Cl	220–380	$-(19.93 \pm 1.8) + 3.65\times10^{-2}(T-300)$	-45.3[d]	-4.23	-15.70
CF_3CN	300–380	$-(20.84 \pm 1.02) + 4.53\times10^{-2}(T-300)$	-39.3[e]	-3.65	-17.19
CF_3Br	300–380	$-(25.92 \pm 0.61) + 5.27\times10^{-2}(T-300)$[a] $+ 8.52\times10^{-4}(T-300)^{2}$[a]	-51.4[f]	-4.81	-21.11
CF_3I	340–380	$-(30.67 \pm 2.08) + 1.4\times10^{-1}(T-340)$	-65.4[g]	-6.11	-24[h]

[a] Reference 15.
[b] C. J. Jameson, A. K. Jameson, and S. M. Cohen, J. Chem. Phys. **67**, 2771 (1977).
[c] L. Petrakis and H. J. Bernstein, J. Chem. Phys. **37**, 2731 (1962).
[d] G. Foex, *Tables de Constantes et Donnees Numerique 7 Constantes Selectionees Diamagnetisme et Paramagnetisme* (Masson et Cie, Paris, 1957).
[e] Calculated from Pascal's constants.
[f] Calculated from Pascal's constants; agrees with -52.6 obtained by Beran and Kevan (Ref. 22) using Haberditzl's method.
[g] Calculated from Pascal's constants, in good agreement with -68.6 calculated (Ref. 22) using Haberditzl's method.
[h] At 340 K. Extrapolated value at 300 K is -30.

between molecules, the rotating CF_3X molecule behaves like a loaded sphere with three identical probes on the surface of the sphere. The differences in mass and polarizability may be enough to give us a better understanding of intermolecular effects by comparing the self σ_1 of the members of the series. Our earlier studies seemed to indicate that CF_3Br was unusual in that the intermolecular effects measured in the liquid phase (from gas-to-liquid shifts) differ significantly from those measured in the dilute gas phase.[15] At that time, it appeared that intermolecular effects on ^{19}F shielding in CF_3Br was qualitatively different from that in CF_3H and CF_3Cl. In the present study of the entire series, we arrive at a better perspective of this difference. We in fact find that there is generally some difference between the binary-only intermolecular effects on shielding measured in the dilute gas phase compared to that including many-body interaction effects measured in the liquid gas phase. We find that the differences are small for H and Cl but larger for Br, I, and CN. In other words the intermolecular effects on ^{19}F shielding in CF_3Br are not qualitatively different from that in the other members of the series, only different in magnitude from the others in the smaller subset previously reported.

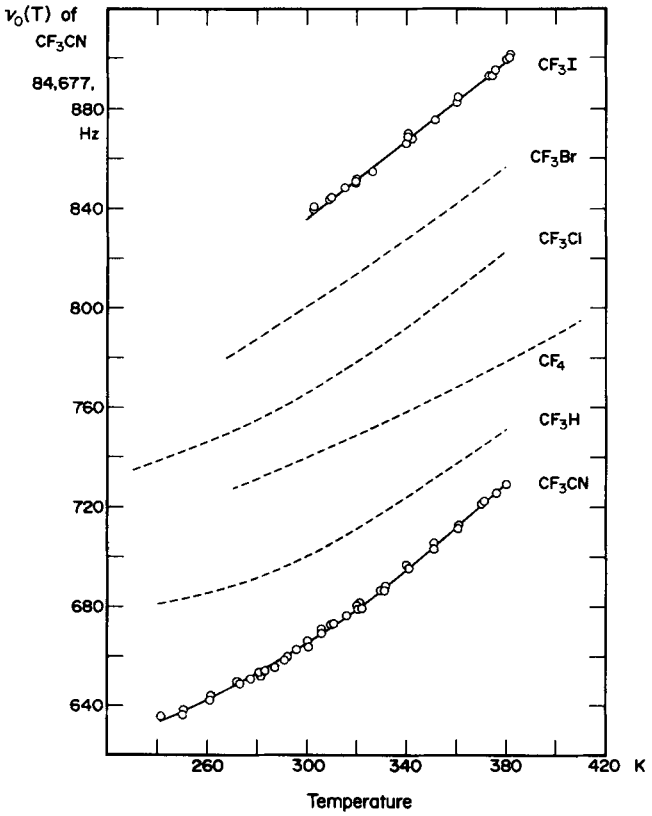

FIG. 2. Temperature dependence of ^{19}F nuclear resonance frequency in the zero-density limit, obtained by subtracting the intermolecular effects. The relative frequency separations between the various ^{19}F chemical environments are not reflected in this figure. The curves are placed in this order solely for comparison of the temperature dependence. The dashed lines are results previously published (Ref. 11) for other members of the CF_3X series. The curves are corrected for the slight temperature dependence of the lock substance. Fitted to quadratic functions of temperature and expressed in ppm, these curves give $[\sigma_0(T) - \sigma_0(300)]$ for the rovibrationally averaged CF_3X molecules (Table II).

EXPERIMENTAL RESULTS

The experimental details have been described in an earlier paper.[16] CF_3I and CF_3CN gases were obtained from PCR Research Chemicals. The typical raw data are shown in Fig. 1 for CF_3CN. A sample of known given density shows a nonlinear increase in ^{19}F resonance frequency with increasing temperature. Samples of different densities have resonance frequencies which are displaced from each other by amounts which vary slightly with temperature, the higher density samples appearing at higher frequencies. At any given temperature these displacements are directly proportional to the density differences between samples. When the curves for different densities are strictly parallel the intermolecular effects are temperature independent (i.e., σ_1 is a constant). Figure 1 shows data which are typical of what we have observed for most gases. When the curves are not exactly parallel, we usually observe that the separation between them increases with decreasing temperature. Below the tem-

TABLE II. Temperature dependence of the ^{19}F nuclear magnetic shielding in the zero-pressure limit.

Molecule	T(K)	$[\sigma_0(T) - \sigma_0(300)]$ (ppb)	
CF_3CN	237–380	$-7.57\,(T-300)$	$-2.12\times10^{-2}\,(T-300)^2$
CF_3I	300–380	$-9.25\,(T-300)$	

perature at which the density of the sample becomes equal to the density of vapor in equilibrium with liquid, a break is observed in the resonance frequency vs T curve. As the temperature is further lowered, the ^{19}F resonance frequency drops to values characteristic of the lower density of the vapor at that temperature. The resonance frequencies of the individual samples (all-gas data only) are least-squares-fitted to a quadratic function of temperature. The frequencies from these best fits are then plotted vs density for chosen temperatures, at 10° intervals. These plots are all linear and their slopes give the values of $\sigma_1(T)$, as in

$$\sigma(T,\rho) = \sigma_0(T) + \sigma_1(T)\rho + \ldots .$$

The σ_1 values are found to be dependent on temperature for CF_3CN and all the other CF_3X (X = H, F, Cl, Br, I). Liquefaction of the CF_3I samples limited the range of temperatures over which σ_1 could be determined; four or more of the samples remained gaseous over the range 330–380 K only. Results are given in Table I.

When $\sigma_1(T)\rho$ (in Hz) is subtracted from each observed resonance frequency (using all of the data points shown in Fig. 1) for CF_3CN, for example) and correction for the temperature dependence of the lock substance is made, the results obtained are as shown in Fig. 2. The resonance frequencies of all the gas samples drop to a common curve $\nu_0(T)$ characteristic of the zero-pressure (zero-density) limit. The vapor data corrected by $\sigma_1(T)\rho_{vap}(T)$ also are included in Fig. 2. The densities of vapor in equilibrium with liquid were obtained from literature values,[17–20] except in the case of CF_3H in which the vapor density was approximated from the vapor pressure.[17]

On the NMR time scale, the observed nuclear shielding is the time average over the molecular rotations and vibrations. Alternatively, one could view $\nu_0(T)$ as an ensemble

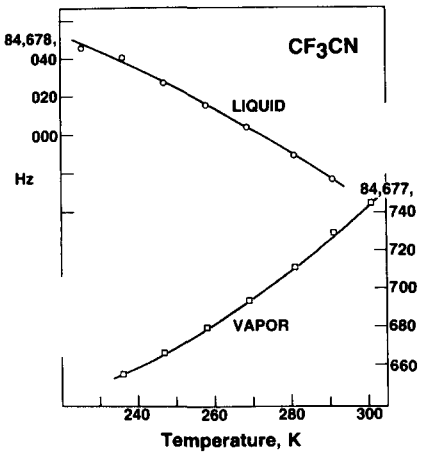

FIG. 3. The resonance frequencies of the liquid phase and the vapor in equilibrium with it can be measured from the same spectrum. A typical result is shown here for CF_3CN. The functions describing these curves for CF_3CN and the other CF_3X molecules are given in Table III.

average, with the shielding characteristic of each rovibrational state weighted according to its population. There is an intrinsic temperature dependence of nuclear magnetic shielding even in the absence of intermolecular interactions for all but monatomic molecules. The present results for CF_3CN and CF_3I are compared with those of CF_3H, F, Cl, and Br[11,12] in Fig. 2. From these $\nu_0(T)$ curves, $[\sigma_0(T)$-$\sigma_0(300)]$ can be obtained as quadratic functions of temperature shown in Table II.

We have also measured the gas-to-liquid shifts for these fluorine nuclei by observing the signal of the equilibrium vapor and the liquid in the same spectrum. The liquid resonance frequency decreases with increasing temperature as the vapor resonance frequency increases. A typical result is shown in Fig. 3 for CF_3CN. These curves are likewise described as quadratic functions of temperature by using a least-squares-fitting routine. The results are given in Table III for the CF_3X molecules (X = H, Cl, Br, I and CN). The shielding difference between liquid and vapor at each temperature is dependent only on the difference in density since the intrinsic temperature dependence of the rovibrationally averaged ^{19}F shielding of a molecule subtracts out. Although the $\sigma_1(T)\rho$ term suffices to describe the observed linear dependence of shielding in the dilute gas [as expected from binary (only) intermolecular interactions], in the liquid phase many-body effects are important, so that the dependence of shielding on the density of the liquid may be more complex. The plots shown in Fig. 4 of the functions $(\sigma_{liq} - \sigma_{vap})(T)$ are a measure of the effects of intermolecular interactions on shielding in this regime. These curves should extrapolate to zero at the critical temperature at which point vapor and liquid become indistinguishable. Figure 4 shows that the curves could plausibly approach zero at the respective critical temperatures 288, 301.9, 340.5, ~386, and 311.1 K[17] for X = H, Cl, Br, I, and CN. The bulk susceptibility contributions to the shielding difference $(\sigma_{liq} - \sigma_{vap})$ are 20%–25% of the observed values. For the sample geometry used here, with the cylindrical sample perpendicular to the magnetic field direction, the bulk susceptibility contribution is $(2\pi\chi/3)(\rho_{liq} - \rho_{vap})(T)$. When the molecular magnetic susceptibility χ is assumed to be temperature independent, these contributions are as given in the last three columns of Table III. The σ_1 values also contain bulk susceptibility contributions $\sigma_{1b} = 2\pi\chi/3$. $(\sigma_1 - \sigma_{1b})$ is the shielding change with density in the limit of the very dilute gas due to pairwise intermolecular interactions. The σ_{1b} part is uninteresting in itself. It is the same for all nuclei in the molecule since it only depends on the molecular magnetic dipole susceptibility. In the case of ^{19}F nuclei in CF_3X, observed in an electromagnet this susceptibility term is roughly one-quarter of the measured σ_1 and is the same sign (a deshielding effect) as the pairwise intermolecular effects.

TABLE III. Temperature dependence of ^{19}F nuclear resonance in the liquid phase and in the vapor in equilibrium with it. The experimental data can be adequately described by the following functions valid only in the temperature ranges indicated:

$$\nu_{vap}(T) = \nu_{vap}(T_0) + b_1(T - T_0) + b_2(T - T_0)^2(\text{Hz}),$$
$$\nu_{liq}(T) = \nu_{liq}(T_0) + a_1(T - T_0) + a_2(T - T_0)^2(\text{Hz}),$$
$$(\sigma_{liq} - \sigma_{vap})(T) = C_0 + C_1(T - T_0) + C_2(T - T_0)^2(\text{ppm}).$$

The gas-to-liquid shifts due to bulk susceptibilities are shown in the same functional form, for the same range of temperatures.

Molecule	T_0	$\nu_{liq}(T)$(Hz)[a] T	a_1	10^3a_2	$\nu_{vap}(T)$(Hz)[a] T	b_1	10^3b_2
CF_3H	280	240–270	−2.413	−18.28	240–270	1.452	10.02
CF_3Cl	280	242–275	−2.108	...	252–300	1.249	...
CF_3CN	280	225–290	−1.216	−3.82	236–301	1.545	6.84
CF_3Br	300	241–300	−1.672	−6.01	241–300	1.899	11.41
CF_3I	300	190–350	−0.752	−2.90	248–331	1.160	4.59

T	$(\sigma_{liq} - \sigma_{vap})(T)$(ppm) C_0	10^2C_1	10^4C_2	Bulk susceptibility contribution[b] to $(\sigma_{liq} - \sigma_{vap})(T)$ d_0	10^2d_1	10^4d_2
240–270	−2.262	4.56	3.33	−0.66	0.78	...
242–275	−3.649	3.92	...	−0.824	1.09	0.69
240–295	−3.329	3.26	1.26	−0.746	0.69	0.28
241–300	−3.964	4.22	2.06	−1.002	0.76	0.32
252–327	−5.305	2.226	0.88	−1.413	0.50	0.18

[a] These have not been corrected for the slight temperature dependence of the lock substance toluene-d_8.
[b] Calculated by $(2\pi/3)\chi(\rho_{liq} - \rho_{vap})(T)$ using χ values given in Table I, liquid and vapor densities from Ref. 17 for CF_3H, CF_3Cl, and CF_3Br, from Ref. 18, for CF_3CN, and from Refs. 19 and 20 for CF_3I.

DISCUSSION

We have determined the effects of intermolecular interaction on ^{19}F nuclear shielding in the series of CF_3X molecules. The two-body interactions decrease the shielding to the extent $(\sigma_1 - \sigma_{1b})\rho$ in the dilute gas. The $(\sigma_1 - \sigma_{1b})$ at 300 K shown in Table III increases monotonically in the sequence H, F, Cl, Br, I viz. −6.76, −8.65, −15.70, −21.11, −30. ppb/amagat, respectively. If the shielding difference between liquid and vapor is divided by the density difference between liquid and vapor, an "effective σ_1" can be obtained for the liquid. Corrected for the bulk susceptibility, this gives $(\sigma_1^{eff} - \sigma_{1b})$ at 300 K = −7.11, −14.37, −12.84, −14.42, and −16.79 for X = H, Cl, CN, Br, and I, to be compared with $(\sigma_1 - \sigma_{1b})$ at 300 K = −6.76, −15.70, −17.19, −21.11, and −30 ppb/amagat, respectively. We note that while the values are probably within experimental error for CF_3H, the discrepancy increases in the sequence Cl, CN, Br, I, being +1.3, +4.3, +6.7 and +13 ppb/amagat, respectively. These numbers are a measure of many-body effects on shielding in the liquid phase at 300 K. They are opposite in sign to the two-body effects, i.e., two-body effects are deshielding but many-body effects appear to be shielding.

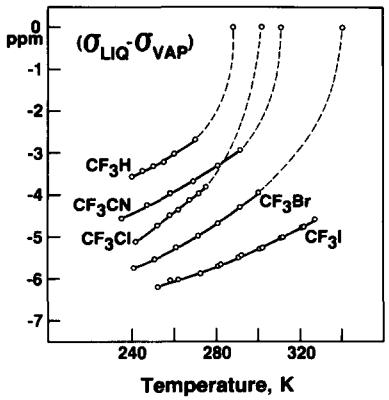

FIG. 4. The gas-to-liquid shifts shown here as $(\sigma_{liq} - \sigma_{vap})(T)$ are due to intermolecular effects and bulk-susceptibility differences between the phases. The latter (given in Table III) constitute 20% to 25% of the observed shifts. These curves should all go to zero at the critical temperature as indicated in the figure for CF_3H (288 K), CF_3Cl (301.93 K), CF_3CN (311.11 K) and CF_3Br (340.5 K). The critical temperature for CF_3I is not available; the value estimated from its boiling point is about 386 K.

The binary collision model of Raynes, Buckingham, and Bernstein[21] relates the $(\sigma_1 - \sigma_{1b})$ to $\sigma_{1w} + \sigma_{1E} + \sigma_{1a}$, the van der Waals, electrical, and magnetic anisotropy effect on shielding respectively. Probably the leading term in σ_1 for ^{19}F in these molecules is σ_{1w}. In the RBB model σ_{1w} has a dispersion contribution of the form $-B\langle R^{-6}\rangle^T\alpha_2 I_1 I_2/(I_1 + I_2)$. If so, then the $(\sigma_1 - \sigma_{1b})$ should be negative and decrease with increasing polarizability. This is indeed the case. The electric dipole polarizabilities α for these molecules are 26.9, 27.3, 45.8, 56.6, and 74.4×10^{-25} cm^3 for X = H, F, Cl, Br, and I, respectively,[22] increasing in the same order as the magnitude of the shielding change due to pairwise interaction $|(\sigma_1 - \sigma_{1b})|$. If there is any effect on $(\sigma_1 - \sigma_{1b})$ due to the loaded sphere aspect of the CF_3X molecules, the $(\sigma_1 - \sigma_{1b})$ values do not reveal it.

The $\sigma_0(T)$ functions are interesting in that they show a systematic ordering of the molecules in their temperature coefficients of shielding. At 300 K, $(d\sigma_0/dT)$ values for CF_3X are -5.60,[11] -5.01,[12] -6.78,[11] -7.75,[11] -9.25, and -7.45 ppb/deg for X = H, F, Cl, Br, I, and CN, respectively. We have found, in a separate study of mean vibrational amplitudes of the C–F bond in these molecules, that the $(\langle \Delta r_{CF} \rangle^T - \langle \Delta r_{CF} \rangle^{300})$ in these molecules increase in the order H, F, Cl, Br, and I as might be expected. These functions change in the series in such a way that we obtain from the observed $[\sigma_0(T) - \sigma_0(300)]$ shown in Fig. 2 empirical $(\partial\sigma^F/\partial\Delta r_{CF})_e$ values in the order X = F, Cl, Br, and I. These calculations are reported elsewhere.[23]

In summary, we have measured the intermolecular effects on ^{19}F nuclear magnetic shielding in the CF_3X series by two methods. The measurements on dilute all-gas samples give $(\sigma_1 - \sigma_{1b})$, the change in nuclear shielding due to binary interactions only. The measurements of gas-to-liquid shifts give an analogous effective value $(\sigma_1^{eff} - \sigma_{1b})$ for the liquid phase. The latter is the change in nuclear shielding with liquid density due to binary and many-body interactions. The many-body effects on nuclear shielding are found to be opposite in sign to the two-body effects. The magnitude of $(\sigma_1 - \sigma_{1b})$ are in the order H, F, Cl, Br, and I. This correlates well with the electric dipole polarizability of these molecules, in agreement with the theory of RBB, implying that the van der Waals dispersion contributions $\sigma_{1\omega}$ are dominant. We have also measured the intrinsic temperature dependence of the ^{19}F nuclear shielding $[\sigma_0(T) - \sigma_0(300)]$. These curves change in a systematic way in the series X = H, F, Cl, Br, and I. By a separate theoretical analysis using the anharmonic force fields for these molecules, it has been shown that magnitudes of the empirically determined $(\partial\sigma^F/\partial\Delta r_{CF})_e$ do increase in the order F, Cl, Br, I.

ACKNOWLEDGMENTS

This research was supported in part by The National Science Foundation (grant CHE81-16193). Some of the data were taken by D. Oppusunggu and J. Honarbakhsh; their assistance is gratefully acknowledged.

[1] S. K. Garg, J. A. Ripmeester, and D. W. Davidson, J. Chem. Phys. **77**, 2847 (1982); **79**, 4101 (1983).
[2] A. B. Harris, E. Hunt, and H. Meyer, J. Chem. Phys. **42**, 2851 (1965).
[3] A. J. Montana, B. R. Appleman, and B. P. Dailey, J. Chem. Phys. **66**, 1850 (1977); C. S. Yannoni, B: P. Dailey, and G. P. Ceasar, *ibid.* **54**, 4020 (1971).
[4] R. Ditchfield, Mol. Phys. **27**, 789 (1974).
[5] S. K. Garg and J. S. Tse, Chem. Phys. Lett. **92**, 150 (1982).
[6] C. J. Jameson, A. K. Jameson, and P. M. Burrell, J. Chem. Phys. **73**, 6013 (1980).
[7] C. J. Jameson, A. K. Jameson, and J. Honarbakhsh (to be published).
[8] A. P. Cox, G. Duxbury, J. A. Hardy, and Y. Kawashima, J. Chem. Soc. Faraday Trans. 2 **76**, 339 (1980).
[9] Y. Kawashima and A. P. Cox, J. Mol. Spectrosc. **7**, 481 (1978).
[10] V. Typke, M. Dakkouri, and H. Oberhammer, J. Mol. Struct. **44**, 85 (1978).
[11] C. J. Jameson, A. K. Jameson, and H. Parker, J. Chem. Phys. **69**, 1318 (1978).
[12] C. J. Jameson, A. K. Jameson, and S. M. Cohen, J. Chem. Phys. **67**, 2771 (1977).
[13] P. Lazzaretti and R. Zanasi, J. Chem. Phys. **75**, 5019 (1981).
[14] M. Schindler and W. Kutzelnigg, J. Am. Chem. Soc. **105**, 1360 (1983).
[15] C. J. Jameson, A. K. Jameson, and H. Parker, J. Chem. Phys. **70**, 5916 (1979).
[16] C. J. Jameson, A. K. Jameson, and D. Oppusunggu (to be published).
[17] *Landolt–Börnstein*, 6th ed. (Springer, Berlin, 1967), Vol. 4, Part 4a.
[18] A. H. N. Mousa, J. Fluorine Chem. **6**, 221 (1975).
[19] E. A. Nodiff, A. V. Grosse, and M. Hauptschein, J. Org. Chem. **18**, 235 (1953).
[20] I. McAlpine and H. Sutcliffe, J. Phys. Chem. **74**, 1422 (1970).
[21] W. T. Raynes, A. D. Buckingham, and H. J. Bernstein, J. Chem. Phys. **36**, 3481 (1962).
[22] J. A. Beran and L. Kevan, J. Phys. Chem. **73**, 3860 (1969).
[23] C. J. Jameson, paper presented at Bryce Crawford, Jr. Symposium, University of Minnesota, May, 1983.